Stochastic analysis of well-type flows in randomly heterogeneous porous formations

Gerardo Severino[1]

Received 2 August 2010; revised 20 December 2010; accepted 6 January 2011; published 18 March 2011.

[1] Well-type flow takes place in a heterogeneous porous formation where the transmissivity is modeled as a stationary *random space function* (RSF). General expressions for the covariances of the head and flux are obtained and analyzed. The second-order approximation of the mean radial flux is represented as the product between the solution $q_r^{(0)}(r)$ valid in a homogeneous domain and a distortion term $\Psi_q(r)$, which adjusts $q_r^{(0)}(r)$ according to the medium heterogeneity. The spatial dependence of the function $\Psi_q(r)$ is studied. In view of the formation identification problem, the equivalent $T^{(\mathrm{eq})}$ and apparent $T^{(\mathrm{ap})}$ transmissivity are computed. The important result is the relationship $T^{(\alpha)}(r) = [1 - \omega^{(\alpha)}(r)]T_H + \omega^{(\alpha)}(r)T_G$ (α may be either "eq" or "ap"), where T_H and T_G represent the harmonic and the geometric means of the transmissivity, respectively. The position-dependent weight $\omega^{(\alpha)}$ is explicitly calculated. Indeed, close to the well, it yields $T^{(\alpha)}(0) = T_H$, which is understandable in view of the fact that the limit $\frac{r}{I} \to 0$ is equivalent to $I \to \infty$, which is the heterogeneity structure of a stratified formation. Nevertheless, the effective transmissivity of a stratified formation is precisely T_H. In contrast, far from the well, one has $T^{(\alpha)}(\infty) = T_G$, with the flow being slowly varying in the mean there. It is shown that $T^{(\alpha)}(r)$ grows with increasing $\frac{r}{I}$. In the case of $T^{(\mathrm{eq})}$, the rate of growing is found (similar to Dagan and Lessoff (2007)) to be strongly dependent upon the position in the flow domain, whereas $T^{(\mathrm{ap})}$ is a more robust property. Finally, it is shown how the general results can be used for practical applications.

Citation: Severino, G. (2011), Stochastic analysis of well-type flows in randomly heterogeneous porous formations, *Water Resour. Res., 47*, W03520, doi:10.1029/2010WR009840.

1. Introduction

[2] Flows generated by single (distributed) sources such as flows toward pumping (injecting) wells are of central interest in hydrology. Many solutions for such flows have been derived for different configurations in homogeneous [*Muskat*, 1937] as well as layered aquifers [e.g., *Neuman and Witherspoon*, 1969]. These solutions have served as a basis for solving many practical problems.

[3] However, natural porous formations are heterogeneous, with their transmissivity varying in the space quite widely [*Dagan*, 1989]. These changes have a significant impact upon water flow [see, e.g., *Neuman and Orr*, 1993]. Since the transmissivity varies in the space in an erratic manner, it is common to model it as a RSF, and to regard the flow equations as stochastic. As a consequence, the head and flux become RSFs as well.

[4] Only recently, problems associated with radially converging (diverging) flows of the kind encountered around extracting (injecting) wells have been tackled. Their analysis to date has been focused mainly on the definition of a proper upscaled transmissivity (for a general discussion on this issue, see *Dagan et al.* [2009]) that would allow one to replace the heterogeneous formation by a homogeneous (fictitious) equivalent formation [*Matheron*, 1967; *Dagan*, 1989; *Gomez-Hernandez and Gorelick*, 1989; *Ababou and Wood*, 1990; *Butler*, 1991; *Naff*, 1991; *Desbarats*, 1992; *Neuman and Orr*, 1993; *Oliver*, 1993; *Indelman et al.*, 1996; *Sanchez-Vila*, 1997; *Riva et al.*, 2001]. Thus, the central problem is the identification of the statistical structure of the transmissivity by the aid of field tests [see, e.g., *Schad and Teutsch*, 1994]. Indeed, by using head measurements, one can infer the transmissivity statistical structure if the theoretical link between the spatial correlation of the flow properties and the transmissivity is available.

[5] The first studies on flow generated by sources of a given flux in randomly heterogeneous porous formations can be traced back to the pioneering work of *Shvidler* [1966]. Analytical results valid in the near and the far fields were obtained by *Dagan* [1982] who, similar to *Shvidler* [1966] and *Matheron* [1967], employed the perturbation approach in the variance of the log transmissivity. Hence, the apparent transmissivity (relating the mean velocity to the mean head gradient) has been obtained as an integral operator, the kernel of which depends upon the transmissivity statistics [*Indelman and Abramovich*, 1994]. Subsequently, *Fiori et al.* [1998] computed the second-order moments of head and flux for steady flow toward a well with a given head. Notwithstanding some simplifying assumptions (such as that of highly anisotropic formation), *Fiori et al.* [1998] were faced with a very heavy numerical

[1]Division of Water Resources Management, University of Naples FEDERICO II, Portici, Italy.

0043-1397/11/2010WR009840

burden. The same problem has been (numerically) investigated by *Riva et al.* [2001]. Their solution was based on recursive approximations of exact nonlocal moment equations developed by *Neuman and Orr* [1993] and *Guadagnini and Neuman* [1999].

[6] In this paper, we are concerned with modeling of steady water flow at regional scale. By regional scale, we refer to entire aquifers (or major parts) that are characterized by horizontal scales much larger than the formation thickness. At this scale, it is customary to model the flow as two dimensional in the horizontal plane by averaging the head and specific discharge over the thickness. The structure of the paper is as follows. In section 2, we formulate the mathematical problem leading to the fluctuations of the head and flux. These fluctuations are used (section 3) to compute the covariance of the head (section 3.1), the flux, and the second-order correction to the mean flux (section 3.2). To apply theoretical results for solving practical problems, we compute (section 4) the equivalent and apparent transmissivity. Results are discussed in section 5, whereas we end up by illustrating (section 6) an application.

2. Problem Statement

[7] A two-dimensional porous formation lies in an unbounded domain Ω. The hydraulic transmissivity $T(\mathbf{x})$ is modeled as a stationary RSF of the position $\mathbf{x} \in \Omega$ with arithmetic mean T_A and a given isotropic correlation function. Flow is generated by a pulselike (Dirac function) extraction of water at a constant specific (i.e., per unit depth) volumetric rate Q. The governing equations are

$$\begin{aligned} \mathbf{q}(\mathbf{x}) &= T(\mathbf{x})\mathbf{E}(\mathbf{x}) \quad \text{(Darcy's law)}, \\ \nabla \cdot \mathbf{q}(\mathbf{x}) &= -Q\delta(\mathbf{x}) \quad \text{(mass conservation law)} \end{aligned} \tag{1}$$

where $\mathbf{q}(\mathbf{x})$ is the flux and $\mathbf{E}(\mathbf{x}) = -\nabla H(\mathbf{x})$ represents the gradient of the head H. Elimination of $\mathbf{q}(\mathbf{x})$ in (1) leads to

$$\nabla \cdot [T(\mathbf{x})\nabla H(\mathbf{x})] = Q\delta(\mathbf{x}). \tag{2}$$

A solution of the stochastic Poisson equation (2) is the random function $H(\mathbf{x})$. For mathematical convenience, we introduce the zero-mean RSF $\varepsilon(\mathbf{x})$ defined as

$$\varepsilon(\mathbf{x}) = 1 - \frac{T(\mathbf{x})}{T_A}, \tag{3}$$

and substitute it into (2) to have

$$\Delta_2 H(\mathbf{x}) = -\nabla \cdot [\varepsilon(\mathbf{x})\mathbf{E}(\mathbf{x})] + \frac{Q}{T_A}\delta(\mathbf{x}). \tag{4}$$

[8] Before going on, it is worth emphasizing that the log transmissivity $Y(\mathbf{x}) = \ln T(\mathbf{x})$ (representing the quantity that is usually regarded as RSF) is uniquely determined via (3) since it results in

$$\begin{aligned} T_A &= T_G \exp\left(\frac{\sigma_Y^2}{2}\right), \quad \sigma_\varepsilon^2 = \exp(\sigma_Y^2) - 1, \\ \rho_\varepsilon(\mathbf{x}) &= \frac{\exp[\sigma_Y^2 \rho_Y(\mathbf{x})] - 1}{\exp(\sigma_Y^2) - 1}, \end{aligned} \tag{5}$$

with σ_ε^2 being the variance of ε, whereas T_G and σ_Y^2 represent the geometric mean and the variance of Y, respectively. More important, it is easily seen from the third expression of (5) that, at the first order in the variance σ_Y^2, the autocorrelation functions of ε and Y coincide, i.e., $\rho_\varepsilon(\mathbf{x}) = \rho_Y(\mathbf{x}) + o(\sigma_Y^4)$. As it will be clearer later on, since all the relevant results of this study are obtained in terms of ρ_ε, it turns out that assuming T (and indeed ε) instead of Y as RSF leads to the same conclusions.

[9] To solve equation (4), the head is expanded into an asymptotic series $H(\mathbf{x}) = \sum_{i=0}^{n} H^{(i)}(\mathbf{x})$, with $H^{(i)} = \mathrm{O}(\varepsilon^i)$. Substituting the expansion into (4), and collecting terms up to the first order, leads to

$$\Delta_2 H^{(0)}(\mathbf{x}) = \frac{Q}{T_A}\delta(\mathbf{x}), \qquad \Delta_2 H^{(1)}(\mathbf{x}) = -\nabla \cdot [\varepsilon(\mathbf{x})\mathbf{E}^{(0)}(\mathbf{x})]. \tag{6}$$

The head distribution $H^{(0)}$ represents a solution to the flow problem in a homogeneous formation, and it is given by

$$H^{(0)}(x) = \frac{Q}{2\pi T_A} \ln\left(\frac{x}{\ell_0}\right). \tag{7}$$

Because of the radial symmetry, $H^{(0)}$ depends only upon the magnitude $x = |\mathbf{x}|$ of the distance from the well, and it is uniquely determined by imposing the condition of its vanishing at a certain distance ℓ_0 from the well. In addition, it is well known that, to allow for a wide applicability of (7) within the flow domain, one has to require that $\ell_0 >> I$. This paper focuses on the flow pattern in the close vicinity of a well, that is, for $r \to 0$. As a consequence, even relatively small (but different from 0) values for the ratio $\frac{\ell_0}{I}$ do not affect results provided that one is mainly concerned with the flow behavior in the close vicinity of the well.

[10] The head fluctuation $H^{(1)}$ satisfies a Poisson-type equation with random forcing term, and it can be expressed (after some straightforward algebraic derivations) in terms of the Green's function $G(x) = \frac{T_A}{Q} H^{(0)}(x)$ as

$$H^{(1)}(\mathbf{x}) = \frac{Q}{T_A} \int_\Omega d\mathbf{x}' \varepsilon(\mathbf{x}') \frac{\partial}{\partial x'_m} G(x') \frac{\partial}{\partial x'_m} G(|\mathbf{x} - \mathbf{x}'|). \tag{8}$$

By the same token as before, we expand in asymptotic series the flux $\mathbf{q}$ and get (from Darcy's law) the following equations for the various terms:

$$\begin{aligned} &\mathbf{q}^{(0)}(\mathbf{x}) = T_A \mathbf{E}^{(0)}(\mathbf{x}), \quad \mathbf{q}^{(n)}(\mathbf{x}) = T_A[\mathbf{E}^{(n)}(\mathbf{x}) - \varepsilon(\mathbf{x})\mathbf{E}^{(n-1)}(\mathbf{x})] \\ &(n = 1, 2, \ldots). \end{aligned} \tag{9}$$

The fluctuation (8), together with (9), enables one to derive moments of the flow variables.

3. Moments of the Flow Variables

[11] In this section, we focus on calculating second-order statistical moments of the head H and flux $\mathbf{q}$ because of their importance in the hydrological applications. Since the transmissivity is modeled as a RSF with isotropic autocorrelation, any change of such moments is because of variations along the radial distance r, solely. In addition, as it will be

clearer later on, moments are computed starting from the expression (8) of the head fluctuation. As a consequence, they do not depend upon the parameter ℓ_0.

3.1. Pressure Head

[12] The head covariance $C_H(\mathbf{r}', \mathbf{r}')$ is obtained by multiplying (8) applied at two different points $\mathbf{r}' \neq \mathbf{r}'$, and subsequently by taking the ensemble average, i.e.,

$$C_H(\mathbf{r}', \mathbf{r}'') = \left\langle H^{(1)}(\mathbf{r}')\, H^{(1)}(\mathbf{r}'')\right\rangle = \frac{Q}{T_A}\int_\Omega \frac{d\bar{\mathbf{r}}}{(2\pi)^2}\frac{\bar{\mathbf{r}}\cdot(\bar{\mathbf{r}}-\mathbf{r}')}{(\bar{r}|\bar{\mathbf{r}}-\mathbf{r}'|)^2} C_{\varepsilon H}(\bar{\mathbf{r}}, \mathbf{r}''). \tag{10}$$

Thus, in order to evaluate $C_H(\mathbf{r}', \mathbf{r}')$, one has to compute the cross correlation $C_{\varepsilon H}(\mathbf{r}', \mathbf{r}'') = \left\langle \varepsilon(\mathbf{r}')\, H^{(1)}(\mathbf{r}'')\right\rangle$ between ε (and therefore T) and the head H. This has been done (see Appendix A for details) for an arbitrary autocorrelation ρ_ε of the RSF $\varepsilon(\mathbf{x})$ with given finite integral scale I, and the final result is

$$C_{\varepsilon H}(r', r'') = \frac{Q\sigma_\varepsilon^2}{2\pi T_A}\Psi(r', r''), \tag{11}$$

$$\Psi(r', r'') = \int_{|r'-r''|}^{\infty} \frac{d\xi\xi\rho_\varepsilon(\xi)}{\xi^2 - r'(r'-r'')} - \int_0^{r'} \frac{d\xi\xi\rho_\varepsilon(\xi)}{\xi^2 - r'(r'-r'')}. \tag{12}$$

By switching to polar coordinates in (10),

$$C_H(r', r'') = \frac{Q}{T_A}\int_0^\infty \frac{d\bar{r}}{(2\pi)^2} C_{\varepsilon H}(\bar{r}, r'') \int_0^{2\pi} \frac{d\theta(\bar{r} - r'\cos\theta)}{\bar{r}^2 + r'^2 - 2r'\bar{r}\cos\theta}, \tag{13}$$

and calculating the inner integral

$$\int_0^{2\pi} \frac{d\theta(\bar{r} - r'\cos\theta)}{\bar{r}^2 + r'^2 - 2r'\bar{r}\cos\theta} = \frac{2\pi}{\bar{r}} h(\bar{r} - r') \tag{14}$$

(h is a Heaviside function defined as $h(x) = 0$ for $x < 0$, $h(x) = \frac{1}{2}$ for x = 0, and h (x) = 1 for x > 0) leads to

$$C_H(r', r'') = \left(\frac{Q\sigma_\varepsilon}{2\pi T_A}\right)^2 \int_{r'}^\infty \frac{d\bar{r}}{\bar{r}}\Psi(\bar{r}, r''). \tag{15}$$

The head variance $\sigma_H^2(r)$ is obtained by setting $r' = r'' = r$ into (15), i.e.,

$$\sigma_H^2(r) = \left(\frac{Q\sigma_\varepsilon}{2\pi T_A}\right)^2 \int_r^\infty \frac{d\bar{r}}{\bar{r}}\Psi(\bar{r}, r). \tag{16}$$

[13] The correction $\langle H^{(2)}(r)\rangle$ to the mean head has been calculated by *Indelman* [2001], and we briefly recall it since it will be used later on. Thus, it is convenient to represent the second-order approximation $\langle H(r)\rangle_2 = H^{(0)}(r) + \sigma_\varepsilon^2\langle H^{(2)}(r)\rangle$ of the mean head as

$$\langle H(r)\rangle_2 = H^{(0)}(r)\Psi_H(r), \qquad \Psi_H(r) = 1 + \sigma_\varepsilon^2\psi_H(r), \tag{17}$$

where $\psi_H(r)$ adjusts the homogeneous head $H^{(0)}$ according to the medium heterogeneity. The function $\psi_H(r)$ has been derived by *Indelman* [2001], and it is written as

$$\psi_H(r) = \frac{1}{2}\left[1 - \frac{\omega(r) - \omega(\ell_0)}{\ln r - \ln \ell_0}\right], \quad \omega(r) = \int_r^\infty \frac{dx}{x}\left(1 - \frac{r^2}{x^2}\right)\rho_\varepsilon(x). \tag{18}$$

It is easy from (18) to investigate the flow behavior in the near and far fields. Indeed, close to the well, one has $\psi_H(0) = \frac{1+\rho_\varepsilon(0)}{2} = 1$. Such a limit clearly differs from that (i.e., $\psi_H(0) = 0$) obtained by *Severino et al.* [2008], who considered a Dirichlet-type condition (i.e., given head) at the well. At the other extreme of large distances, one has $\psi_H(\infty) = \frac{1+\rho_\varepsilon(\infty)}{2} = \frac{1}{2}$. Since this result coincides with that obtained by *Severino et al.* [2008], it is seen that the type of the boundary condition at the well does not affect $\psi_H(r)$ in the far field.

3.2. Flux

[14] The leading-order term $q_r^{(0)}$ and the fluctuation $\mathbf{q}^{(1)}$ of the flux are obtained from (9) as follows:

$$q_r^{(0)}(r) = \frac{Q}{2\pi r}, \qquad \mathbf{q}^{(1)}(\mathbf{r}) = T_A[\mathbf{E}^{(1)}(\mathbf{r}) - \varepsilon(\mathbf{r})\mathbf{E}^{(0)}(\mathbf{r})]. \tag{19}$$

The flux covariance along radii, i.e., $C_q(\mathbf{r}', \mathbf{r}'') = \left\langle q_r^{(1)}(\mathbf{r}')\, q_r^{(1)}(\mathbf{r}'')\right\rangle$ (with $q_r^{(1)}$ being the fluctuation of the radial component of the flux), can be written as

$$\frac{C_q(\mathbf{r}', \mathbf{r}'')}{T_A^2} = C_q^{(\infty)}(\mathbf{r}', \mathbf{r}'') - \tilde{C}_q(\mathbf{r}', \mathbf{r}'') + C_{E_r}(\mathbf{r}', \mathbf{r}''), \tag{20}$$

$$C_q^{(\infty)}(\mathbf{r}', \mathbf{r}'') = \left(\frac{Q\sigma_\varepsilon}{2\pi T_A}\right)^2 \frac{\rho(|\mathbf{r}' - \mathbf{r}''|)}{r'r''}, \tag{21}$$

$$\tilde{C}_q(\mathbf{r}', \mathbf{r}'') = \frac{Q}{2\pi T_A}\left[\frac{1}{r'}\frac{\partial}{\partial r''} C_{\varepsilon H}(\mathbf{r}', \mathbf{r}'') + \frac{1}{r''}\frac{\partial}{\partial r'} C_{\varepsilon H}(\mathbf{r}'', \mathbf{r}')\right]. \tag{22}$$

The quantity $C_{E_r}(\mathbf{r}', \mathbf{r}'') = \left\langle \frac{\partial}{\partial r'}H^{(1)}(\mathbf{r}')\frac{\partial}{\partial r''}H^{(1)}(\mathbf{r}'')\right\rangle$ represents the head-gradient covariance. The usefulness of the decomposition (20) relies on the fact that one can clearly distinguish the contribution of the mean radial flow (i.e., $C_q^{(\infty)}$) from those related to the head-gradient fluctuation. Computing $\tilde{C}_q(\mathbf{r}', \mathbf{r}'')$ and $C_{E_r}(\mathbf{r}', \mathbf{r}'')$ requires multidimensional numerical quadratures [*Fiori et al.*, 1998; *Riva et al.*, 2001; *Guadagnini et al.*, 2003]. Such a computational burden was circumvented by *Indelman and Dagan* [1999] by taking advantage of the highly anisotropic geometry of sedimentary formations. This assumption is also equivalent to approximating the fluctuation of the flux (second expression of (19)) with

$$\mathbf{q}^{(1)}(\mathbf{r}) \approx -T_A\varepsilon(\mathbf{r})\,\mathbf{E}^{(0)}(\mathbf{r}). \tag{23}$$

[15] Turning to the problem of computing $\tilde{C}_q(\mathbf{r}', \mathbf{r}'')$, insertion of (11) into (22) and carrying out the required differentiations leads to

$$\tilde{C}_q(r', r'') = -2\overline{C}_q^{(\infty)}(r', r'') - \left(\frac{Q\sigma_\varepsilon}{2\pi T_A}\right)^2 [\Phi(r', r'') + \Phi(r'', r')], \tag{24}$$

$$\Phi(x,y)=\int_{|x-y|}^{\infty}\frac{d\xi\xi\rho_\varepsilon(\xi)}{\left[\xi^2-x(x-y)\right]^2}-\int_0^x\frac{d\xi\xi\rho_\varepsilon(\xi)}{\left[\xi^2-x(x-y)\right]^2}, \quad (25)$$

where $\overline{C}_q^{(\infty)}(x,y)=C_q^{(\infty)}(x,y)$ for $x\neq y$, and $\overline{C}_q^{(\infty)}(x,x)=\frac{1}{2}\overline{C}_q^{(\infty)}(x,x)$. The head-gradient covariance $C_{E_r}(\mathbf{r}',\mathbf{r}'')=\frac{\partial^2}{\partial r'\partial r''}\left\langle H^{(1)}(\mathbf{r}')H^{(1)}(\mathbf{r}'')\right\rangle$ is easily obtained from (15) after carrying out the derivatives with respect to r' and r''. The result is

$$C_{E_r}(r',r'')=\overline{C}_q^{(\infty)}(r',r'')+\left(\frac{Q\sigma_\varepsilon}{2\pi T_A}\right)^2\Phi(r',r''). \quad (26)$$

Thus, by accounting for (20), (21), (24), and (26), we end up with the following expression for the flux covariance:

$$C_q(r',r'')=\left(\frac{Q\sigma_\varepsilon}{\pi}\right)^2\left[\frac{\rho_\varepsilon(r'-r'')}{r'r''}+\frac{1}{2}\Phi(r',r'')+\frac{1}{4}\Phi(r'',r')\right]. \quad (27)$$

The covariance (27), which represents one of the main results of this paper, is given in terms of one quadrature (which is easily computed after specifying the shape of ρ_ε). In particular, the variance $\sigma_q^2(r)=C_q(r,r)$ is

$$\sigma_q^2(r)=\left(\frac{Q\sigma_\varepsilon}{2\pi r}\right)^2\left[\frac{5}{2}+3\psi_q(r)\right],\qquad \psi_q(r)=r^2\int_r^\infty dx\frac{\rho_\varepsilon(x)}{x^3}. \quad (28)$$

[16] In some hydrological applications (such as delimiting the protection zone of pumping wells), it would be desirable to determine the distribution of the mean radial flux. At σ_ε^2 order, the mean radial flux results from truncating the asymptotic expansion (9) at the second term, and subsequently taking the expectation, i.e., $\langle q_r(r)\rangle_2=q_r^{(0)}(r)+\langle q_r^{(2)}(r)\rangle$, where (see equation (9))

$$q_r^{(0)}(r)=T_AE^{(0)}(r)=\frac{Q}{2\pi r},\qquad \langle q_r^{(2)}(r)\rangle=T_A[\langle E^{(2)}(r)\rangle-\sigma_{\varepsilon E}(r)]. \quad (29)$$

In equation (29), the mean second-order gradient is given by (see equation (17))

$$\langle E^{(2)}(r)\rangle=-\sigma_\varepsilon^2\frac{\partial}{\partial r}[H^{(0)}(r)\psi_H(r)], \quad (30)$$

whereas the cross variance is obtained by taking $r'=r''=r$ into $\left\langle\varepsilon(\mathbf{r}')\frac{\partial}{\partial r''}H^{(1)}(\mathbf{r}'')\right\rangle$. Similar to the head, to focus on the impact of the heterogeneity, it is useful to represent (we skip the algebraic derivations) the second-order approximation of the mean flux as

$$\langle q_r(r)\rangle_2=q_r^{(0)}(r)\Psi_q(r),\qquad \Psi_q(r)=1+\sigma_\varepsilon^2\left[\frac{1}{2}+2\psi_q(r)\right]. \quad (31)$$

In this way, $\langle q_r(r)\rangle_2$ is expressed as the product between the zero-order term $q_r^{(0)}(r)$ (valid for homogeneous media) and the characteristic heterogeneity function $\Psi_q(r)$, which adjusts $q_r^{(0)}$ according to the medium heterogeneity. Similar to the head, the near and far fields of $\Psi_q(r)$ are easily derived from (31). Thus, from the second expression of (28), it is seen that

$$\lim_{r\to0}\psi_q(r)=\frac{\rho_\varepsilon(0)}{2}=\frac{1}{2},\qquad \lim_{r\to\infty}\psi_q(r)=\frac{\rho_\varepsilon(\infty)}{2}=0. \quad (32)$$

Substituting these limits into (31) leads to

$$\Psi_q(0)=1+\frac{3}{2}\sigma_\varepsilon^2,\qquad \Psi_q(\infty)=1+\frac{\sigma_\varepsilon^2}{2}. \quad (33)$$

[17] Thus, the distortion effect as a result of the medium heterogeneity is higher at the well. This is understandable because of the large variability of q_r in the vicinity of the well. Such a result has important implications in the analysis of tracer tests. Indeed, it has been invoked by *Indelman and Dagan* [1999] to explain the differences in the macrodispersivity coefficient that one has when comparing transport generated by diverging radial flows with that taking place in mean uniform flows.

4. Equivalent Versus Apparent Transmissivity

[18] Traditionally, the transmissivity can be upscaled under conditions of mean uniform gradient. In this case, one ends up with the effective transmissivity T^{ef}, which is a medium property [see, e.g., *Rubin*, 2003]. In our case, the strong nonuniformity in the region adjacent to the well defies the use (in a traditional sense) of the effective transmissivity approach.

[19] It has been shown by *Indelman and Abramovich* [1994] that the upscaled Darcy's law (representing the relationship between mean head and mean gradient) can be defined in a convolution form, the kernel of which depends upon the statistics of the transmissivity. However, direct identification of the kernel by field data seems to be a difficult task (see, also, discussion in the work of *Tartakovsky and Neuman* [1998]). To achieve simple (although approximate) results, one can define various quantities that are expressed in terms of parameters that can be easily measured [e.g., *Tartakovsky et al.*, 2002]. Thus, the concept of equivalent transmissivity (ET) has been introduced [*Matheron*, 1967; *Indelman et al.*, 1996; *Indelman and Zlotnik*, 1997; *Riva et al.*, 2001] in order to relate measured data to the statistical structure of the formation.

[20] Starting from the classical definition of transmissivity for a homogeneous medium, i.e., $T_A=Q\frac{G^{(0)}(r)}{H^{(0)}(r)}$, we define the ET (hereafter denoted by $T^{(\mathrm{eq})}$) as the one pertaining to a fictitious homogeneous medium that conveys the same specific volumetric rate Q as the actual heterogeneous formation, i.e.,

$$T^{(\mathrm{eq})}(r)=Q\frac{G^{(0)}(r)}{\langle H(r)\rangle_2}=T_A\frac{H^{(0)}(r)}{\langle H(r)\rangle_2}=T_A[1+\sigma_\varepsilon^2\psi_H(r)]^{-1}, \quad (34)$$

being the last passage obtained by means of the representation (17). The advantages of equation (34) are as follows: (1) $T^{(\mathrm{eq})}$ can be quantified by pressure-head measurements, and (2) it is useful for scenario simulations by replacing

blocks of heterogeneous media by homogeneous media in numerical computations. Instead, the main limitation of the ET concept is that it depends upon the flow configuration and, therefore, it cannot be considered as a medium property.

[21] A different characterization of the mean flow can be obtained by using the definition of apparent transmissivity (AT). This is defined as the ratio between $\langle q_r \rangle_2$ and $\langle E(r) \rangle_2$, i.e.,

$$T^{(\mathrm{ap})}(r) = \frac{\langle q_r(r) \rangle_2}{\langle E(r) \rangle_2}. \tag{35}$$

[22] Thus, the AT is the property regarded as the effective one by a naive observer that simultaneously measures the mean flux and the mean head gradient. The main advantage of the characterization by $T^{(\mathrm{ap})}$ is that it can be defined in a unique manner. It can be used in more complex domains to delimit the zone in which the effective medium theory applies. To the contrary, the main limitation of such a concept is that it depends on quantities (such as the mean head gradient) that cannot be easily measured. Substitution of $\langle q_r(r) \rangle_2 = \Psi_q(r) q_r^{(0)}(r)$ into (35), and computing the mean gradient $\langle E \rangle_2$, leads to

$$T^{(\mathrm{ap})}(r) = T_A \frac{2 + \sigma_\varepsilon^2 [1 + 4\psi_q(r)]}{2 + \sigma_\varepsilon^2 [1 + 2\psi_q(r)]}. \tag{36}$$

The most important implication (in view of the identification problem) of equation (36) is that now one can relate $T^{(\mathrm{ap})}$ to the characteristic function ψ_q. As a consequence, once ψ_q has been calibrated via the head measurements in the field, one can easily infer the spatial structure of $T^{(\mathrm{ap})}$. The utility of such a result for the practical applications will be illustrated next.

[23] The general representations (34) and (36), together with the results established in the previous sections, lead to the following asymptotics:

$$T^{(\mathrm{eq})}(0) = T^{(\mathrm{ap})}(0) \approx T_H, \qquad T^{(\mathrm{eq})}(\infty) = T^{(\mathrm{ap})}(\infty) \approx T_G, \tag{37}$$

where the last passages have been obtained by accounting for the relationships $T_A = T_G \sqrt{1 + \sigma_\varepsilon^2}$ and $T_G = T_H \sqrt{1 + \sigma_\varepsilon^2}$. The near-field localization by the harmonic mean $T_H = \left\langle \frac{1}{T(\mathbf{x})} \right\rangle^{-1}$ is because of the condition of constant specific volumetric rate Q at the well. Indeed, at the radius scale (i.e., for $r \ll I$), Q is constant, and from the Darcy's law one has

$$\frac{Q}{2\pi r} T^{-1} = \frac{d}{dr} H(r). \tag{38}$$

Then, by writing the local head as $H(r) = \langle H(r) \rangle + H^{(1)}(r)$, and taking the expectation into (38), leads to T_H. In a different way, we could say that, for a local observer at r scale, the condition $\frac{r}{I} \to 0$ is equivalent to $I \to \infty$, which represents the heterogeneity structure of a stratified formation. Nevertheless, the transmissivity of a stratified formation is precisely T_H [*Dagan*, 1982]. In contrast, if the head is prescribed at the well, the same procedure as above shows that the localization is by the arithmetic mean T_A. As for the far field, the flow there behaves as a uniform one [see, e.g., *Indelman and Abramovich*, 1994] for which the transmissivity is $T^{ef} = T_G$.

5. Discussion of Results

[24] In this section, we are going to discuss the general results obtained so far.

5.1. Pressure Head

[25] Starting from the head variance (16), it can be evaluated once the function $\Psi(x, r)$ (which, in turn, depends upon the autocorrelation function of ε) is specified. In particular, substituting the exponential model $\rho_\varepsilon(x) = \exp(-x)$ (we consider the lengths normalized by I, although for simplicity we retain the same notation) in equation (12) leads to

$$\Psi(x, r) = \frac{1}{2} \left\{ \exp\left[-\sqrt{x(x-r)} \right] \Upsilon_1(x, r) + \exp\left[\sqrt{x(x-r)} \right] \Upsilon_2(x, r) \right\}, \tag{39}$$

$$\Upsilon_1(x, r) = \mathrm{Ei}\left[\sqrt{x(x-r)} \right] - \mathrm{Ei}\left[\sqrt{x}(\sqrt{x-r} - \sqrt{x}) \right] - \mathrm{Ei}\left[\sqrt{x-r}(\sqrt{x} - \sqrt{x-r}) \right], \tag{40}$$

$$\Upsilon_2(x, r) = \mathrm{Ei}\left[-\sqrt{x(x-r)} \right] - \mathrm{Ei}\left[-\sqrt{x}(\sqrt{x-r} + \sqrt{x}) \right] - \mathrm{Ei}\left[-\sqrt{x-r}(\sqrt{x} + \sqrt{x-r}) \right], \tag{41}$$

whereas, for Gaussian $\rho_\varepsilon(x) = \exp\left(-\frac{\pi}{4} x^2\right)$, it yields

$$\Psi(x, r) \frac{1}{2} \exp\left[-\frac{\pi}{4} x(x-r) \right] \left\{ \mathrm{Ei}\left[\frac{\pi}{4} x(x-r) \right] - \mathrm{Ei}\left[\frac{\pi}{4} r(x-r) \right] - \mathrm{Ei}\left(-\frac{\pi}{4} xr \right) \right\}. \tag{42}$$

The scaled variance $\overline{\sigma}_H^2(r) = \left(\frac{T_A \sigma_H}{Q \sigma_\varepsilon} \right)^2$ is depicted in Figure 1 as function of the dimensionless distance $\frac{r}{I}$ from the well. In the far field, the head variance is quite low, since the flow practically behaves as a homogeneous flow. The head variance in the far field is easily studied by considering that, for a local observer (i.e., at fixed r), the condition $r \gg I$ is equivalent to $I \to 0$. As a consequence, we can replace the autocorrelation of ε with a white noise signal, i.e., $\rho_\varepsilon \approx \delta$. This line of attack was adopted by *Dagan* [1982] who found (see equation (140) of *Dagan* [1982]) that

$$\overline{\sigma}_H^2(r) \approx \frac{\ln(r/I)}{(2\pi r/I)^2}, \qquad r \gg I. \tag{43}$$

By comparing (see Figure 1) the asymptotic (43) with our general solution, it is seen that the asymptotic of *Dagan* [1982] applies for $r \geq 10I$.

[26] From the point of view of the applications, the near-field behavior is more interesting. The head variance $\overline{\sigma}_H^2(r)$ is singular at $r = 0$. In fact, close to the well, the formation appears as a homogeneous block with harmonic transmissivity T_H. Thus, because of the singular nature of the head

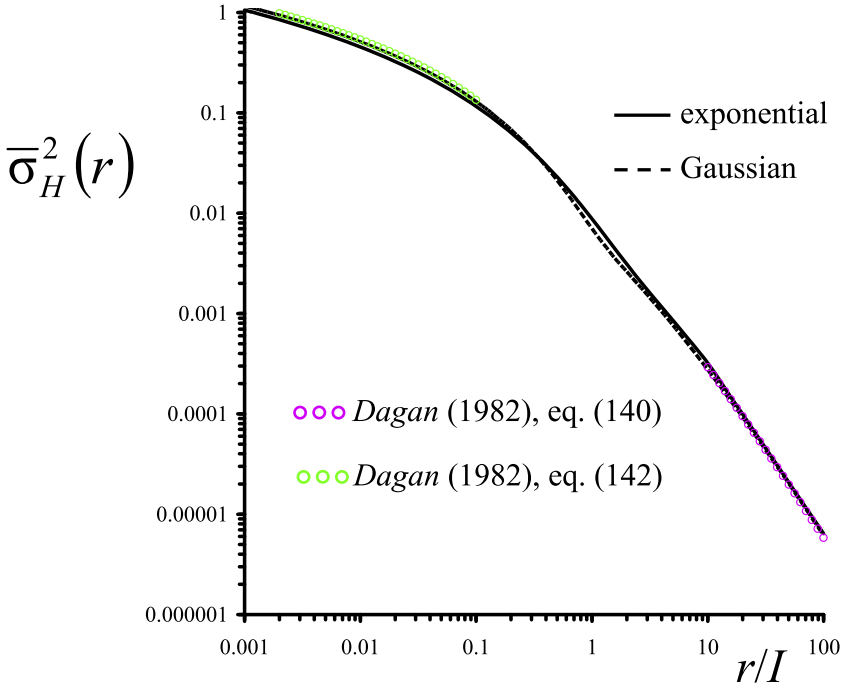

Figure 1. Dimensionless head variance $\overline{\sigma}^2_H$ versus the normalized radial distance $\frac{r}{I}$

there (see equation (7)), the same is true for the variance σ^2_H. Such a result has also been recovered via Monte Carlo simulations [*Riva et al.*, 2001]. The near-field behavior can be studied by assuming $\rho_\varepsilon(x) = 1$ (which is a reasonable approximation in view of the assumption $r \ll I$). This approach has been employed by *Dagan* [1982], and the final result [*Dagan*, 1982, equation (142)] is

$$\overline{\sigma}^2_H(r) \approx \left[\frac{1}{2\pi}\ln\left(\frac{r}{I}\right)\right]^2, \qquad r \ll I. \tag{44}$$

[27] Inspection from Figure 1 shows that the approximation (44) is in a very good agreement with the general expression (16) up to $r \approx 0.1I$. The transitional regime (i.e., $0.1I \leq r \leq 10I$) is computed after insertion of equations (39) and (41). The most evident feature is that the shape of the autocorrelation is practically immaterial.

[28] It is interesting to note from (44) that the coefficient of variation $\mathrm{CV}_H(r) = \frac{\sigma_H(r)}{H^{(0)}(r)} = \sigma_\varepsilon \frac{\overline{\sigma}_H(r)}{G(r)}$ of the head is given by

$$\mathrm{CV}_H(r) \approx \sigma_\varepsilon \left[1 - \frac{\ln(\ell_0/I)}{\ln(r/I)}\right]^{-1}, \qquad \frac{r}{I} \leq 0.1. \tag{45}$$

[29] This result shows that, at the well (i.e., for $r \to 0$), the prediction upon the head is highly uncertain, irrespective of $\frac{\ell_0}{I}$. This is because of the fact that most of the head buildup takes place in a homogeneous inclusion surrounding the well [*Dagan*, 1982]. An important issue concerning the identification of the transmissivity by means of head data attains the optimal location of the piezometers. Indeed, measurements very close to the well would be highly uncertain, whereas in the far field the homogeneous head $H^{(0)}$ is no longer of practical use (because of its logarithmic growth). Thus, a suitable annular sampling region should be properly designed (a wide discussion on such an issue is provided by *Guadagnini et al.* [2003]). For instance, the external radius is determined by the reliability/applicability of the far-field expression of the head, whereas the inner radius could be determined to avoid large uncertainty in the head measurements. To discuss this issue in a quantitative manner, in Figure 2 we have depicted the autocorrelation coefficient of the head $\rho_H(r', r'') = \frac{C_H(r', r'')}{\sigma^2_H(r')}$ versus the dimensionless distance $\frac{r'}{I}$ and some values of $\frac{r''}{I}$. For small r'', the head measurements are correlated over larger distances. This is understandable since, for small r'', the impact of the boundary condition at the well is felt within a large portion of the flow domain. As r'' increases, head measurements at different radial distances are less correlated because of the reduction of the conditioning effect of the boundary condition. In particular, $\rho_H(r', r'')$ tends to become more and more symmetric as r'' increases. This is explained by recalling that, in the far field, the flow behaves as a mean uniform flow for which it is known that the autocorrelation of the flow variables is a symmetric function of the position. It is worth noting that the higher values of ρ_H are attained for the smaller values of the reference distance r'', and vice versa. In fact, the smaller r'', the more persistent the covariance $C_H(r', r'')$ is. Nevertheless, the head variance σ^2_H reduces (with logarithmic law) with r'. Thus, the global effect upon $\rho_H(r', r'') = \frac{C_H(r', r'')}{\sigma^2_H(r')}$ is an increase of the autocorrelation. As soon as the covariance starts to reduce (since head measurements become more and more uncorrelated), then ρ_H drastically decays. To the contrary, for large r'', the covariance decays more rapidly with r' and the overall effect is that ρ_H is smaller.

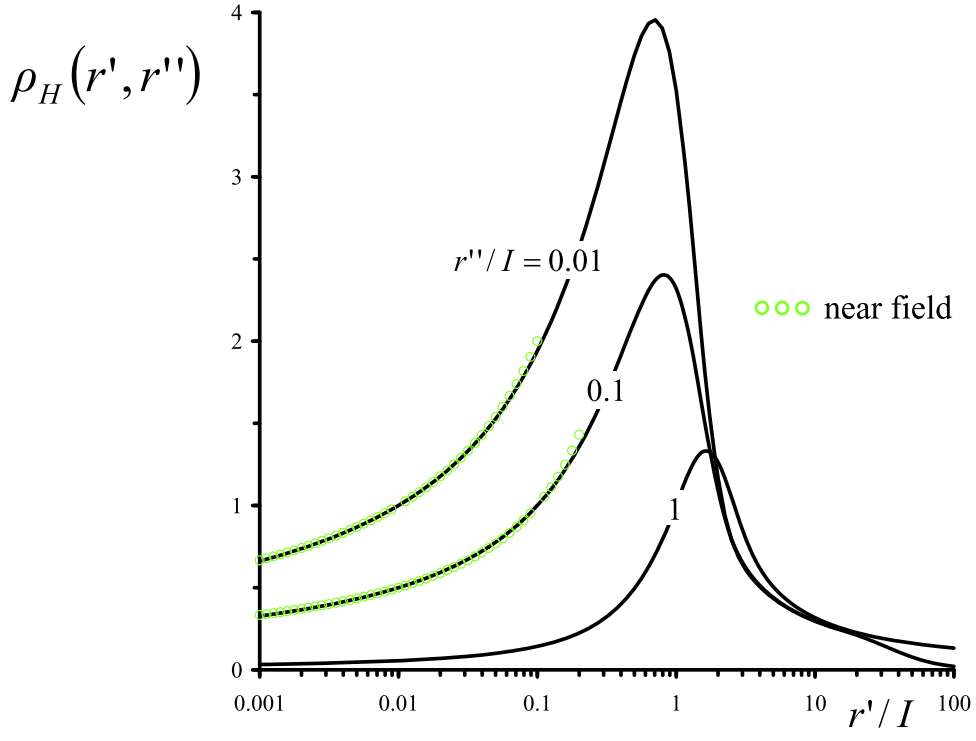

Figure 2. Correlation coefficient $\rho_H(r', r'')$ of the head versus the distance $\frac{r'}{I}$ and different values of $\frac{r''}{I}$.

[30] A simple (approximate) expression for C_H (and therefore for ρ_H) valid in the near field can be obtained. Indeed, by employing the definition of the head covariance $C_H(\mathbf{r}', \mathbf{r}'') = \langle H^{(1)}(\mathbf{r}')H^{(1)}(\mathbf{r}'')\rangle$ and accounting for (8), it is easy to show that $C_H(\mathbf{r}', \mathbf{r}'') = \left(\frac{Q\sigma_\varepsilon}{T_A}\right)^2 \overline{C}_H(\mathbf{r}', \mathbf{r}'')$, being

$$\overline{C}_H(\mathbf{r}', \mathbf{r}'') = \int_\Omega d\mathbf{x}' \frac{\partial}{\partial x'_m} G(x') \frac{\partial}{\partial x'_m} G(|\mathbf{r}' - \mathbf{x}'|) \int_\Omega d\mathbf{x}'' \rho_\varepsilon(\mathbf{x}' - \mathbf{x}'') \times \frac{\partial}{\partial x''_n} G(x'') \frac{\partial}{\partial x''_n} G(|\mathbf{r}'' - \mathbf{x}''|). \tag{46}$$

Close to the well, one may assume that $\rho_\varepsilon \approx 1$ and, therefore, (46) is written as

$$\overline{C}_H(\mathbf{r}', \mathbf{r}'') \approx F(\mathbf{r}')F(\mathbf{r}''), \qquad F(\mathbf{r}) = \int_\Omega d\mathbf{x} \frac{\partial}{\partial x_m} G(x) \frac{\partial}{\partial x_m} G(|\mathbf{r} - \mathbf{x}|). \tag{47}$$

The integral F, also encountered in the electric crystal problem [*Lifshitz and Rozentsveig*, 1946], was calculated by *Indelman* [2001] when analyzing the mean head in a source flow, with the final result being $F(r) = -[G(r) + \frac{r}{2}\frac{d}{dr}G(r)]$. Thus, the near-field approximation of ρ_H is written as

$$\rho_H(r', r'') \approx \frac{\ln(r''/I)}{\ln(r'/I)}. \tag{48}$$

The asymptotic (48) is in excellent accordance (see Figure 2) with the general expression of ρ_H up to $r' \approx 0.1I$ (in the far field, it is found that $\rho_H \approx 0$).

5.2. Flux

[31] Although the general expression for the flux variance has been already obtained (see equation (28)), it is instrumental to re-derive it in a different manner. Thus, we note that the fluctuation $\mathbf{q}^{(1)}$ satisfies the divergent-free condition (the second expression of (1))

$$\frac{\partial}{\partial x_i} q_i^{(1)}(\mathbf{x}) = 0. \tag{49}$$

Hence, switching to polar coordinates in (49), multiplying both sides by $q_r^{(1)}(r)$, and taking the ensemble average leads to

$$\left(\frac{d}{dr} + \frac{2}{r}\right) \sigma_q^2(r) = 0 \quad \Rightarrow \quad \sigma_q^2(r) = \mathrm{O}(r^{-2}). \tag{50}$$

The decay of the flux variance as r^{-2} was known to be asymptotically valid [*Matheron*, 1967; *Shvidler*, 1985; *Naff*, 1991]. Here, it is extended to the entire flow domain. Another issue is about the singular behavior of σ_q^2 at $r = 0$. Indeed, the condition of mass conservation at the well requires that $2\pi rq = Q = \text{constant}$. As a consequence, the flux becomes exceedingly high for $r \to 0$. Thus, the large variance of the specific flux occurring at the well suggests that large sample sizes are necessary to construct reliable statistics from velocity measurements (obtained by flowmeters).

[32] To quantify the uncertainty of the flux, it is convenient to consider the coefficient of variation $\mathrm{CV}_q(r) = \frac{\sigma_q(r)}{q_r^{(0)}(r)}$, which is given (see equations (19) and (28)) by

$$\mathrm{CV}_q(r) = \sigma_\varepsilon \left[\frac{5}{2} + 3\psi_q(r)\right]^{1/2}. \tag{51}$$

[33] By accounting for (32), the following general asymptotics are easily established:

$$\lim_{r\to 0} \mathrm{CV}_q(r) = 2\sigma_\varepsilon, \qquad \lim_{r\to\infty} \mathrm{CV}_q(r) = \sqrt{\frac{5}{2}}\sigma_\varepsilon \tag{52}$$

The condition $\mathrm{CV}_q(\infty) < \mathrm{CV}_q(0)$ is explained by the very large variations of local fluxes at the well, whereas in the far field the flux is slowly varying. These asymptotics may represent useful information for some practical applications, such as the identification of the formation heterogeneity structure (see discussion from *Indelman* [2001]).

[34] The transitional regime of (51) is evaluated after computing $\psi_q(r)$ for a given autocorrelation ρ_ε. By assuming the exponential and the Gaussian models, one has

$$\psi_q(r) = \frac{1}{2}\begin{cases} (1-r)\exp(-r) - r^2\mathrm{Ei}(-r) & \text{(exponential)} \\ \exp\left(-\frac{\pi}{4}r^2\right) + \frac{\pi}{4}r^2\mathrm{Ei}\left(-\frac{\pi}{4}r^2\right) & \text{(Gaussian).} \end{cases} \tag{53}$$

The scaled coefficient of variation $\frac{\mathrm{CV}_q(r)}{\sigma_\varepsilon}$ is depicted in Figure 3 versus the normalized distance $\frac{r}{I}$ from the well. As previously established, CV_q decreases like r^{-1} with $\frac{r}{I}$, and it reaches the large-distance asymptotic after 10 integral scales. The same behavior is observed in the work of *Naff* [1991, Figure 4] in the case $\mu = 10$ (resembling the two-dimensional formation). The near- and far-field values reported by *Naff* [1991] are smaller than those obtained in our case. Indeed, unlike *Naff* [1991] (who considered a three-dimensional domain), in our case fluid particles can circumvent inclusions of low conductivity only laterally (since the aquifer is two dimensional), therefore causing them to depart (from the mean trajectory) to a larger extent.

[35] In view of the analysis of tracer transport, it useful to consider the autocorrelation coefficient ρ_q of the flux. In Figure 4, we have depicted $\rho_q(r', r'') = \frac{C_q(r', r'')}{\sigma_q^2(r')}$ versus the dimensionless distance $\frac{r'}{I}$ and a few values of $\frac{r''}{I}$. For convenience, we have considered the case of Gaussian ρ_ε (the same conclusions can be drawn by dealing with exponential ρ_ε), for which the quadrature (25) is analytically computed, i.e.,

$$\Phi(r', r'') = \frac{\rho_\varepsilon(r')}{2r'r''} - \frac{r'\rho_\varepsilon(r'-r'') - r''}{2r'r''(r'-r'')} - \frac{\pi}{8}\exp\left[-\frac{\pi}{4}r'(r'-r'')\right]\overline{\Phi}(r', r''), \tag{54}$$

$$\overline{\Phi}(r', r'') = \mathrm{Ei}\left[-\frac{\pi}{4}r'(r''-r')\right] - \mathrm{Ei}\left[-\frac{\pi}{4}r''(r''-r')\right] - \mathrm{Ei}\left(-\frac{\pi}{4}r'r''\right). \tag{55}$$

It is seen that flux (similar to the head) values are more correlated when r'' is close to the well because of the conditioning effect of the boundary condition. The most interesting feature is that ρ_q vanishes after five integral scales. In other words, by this distance, the flow becomes slowly varying. This argument was invoked by *Indelman and Dagan* [1999] to justify the approximate velocity covariance that they used to model tracer macrodispersion. On the basis of numerical simulations [see *Indelman and*

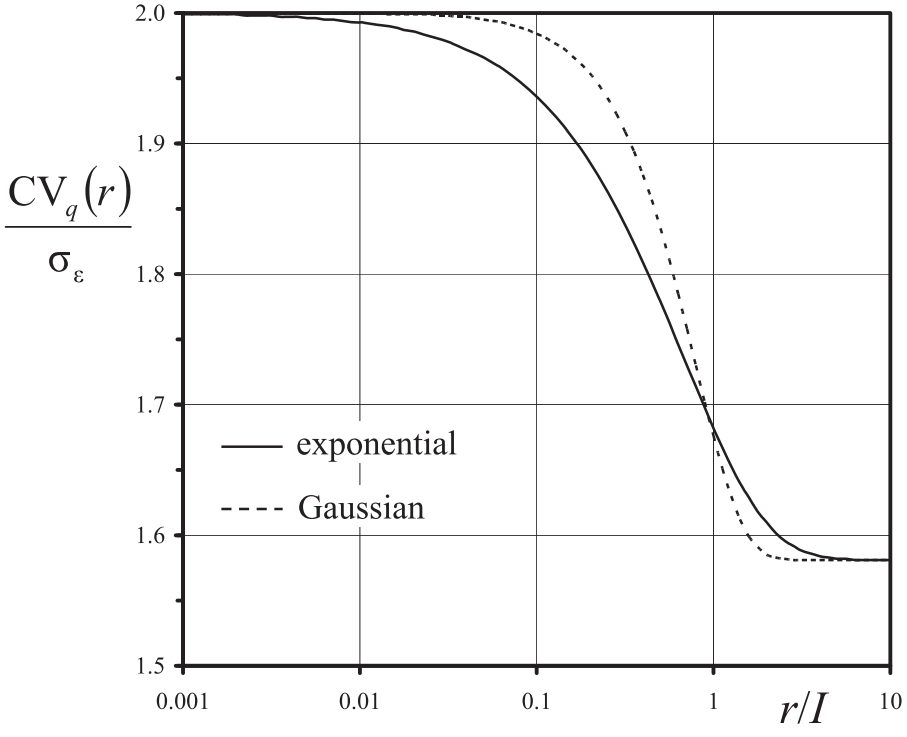

Figure 3. Scaled coefficient of variation $\frac{\mathrm{CV}_q}{\sigma_\varepsilon}$ of the flux versus the normalized radial distance from the well.

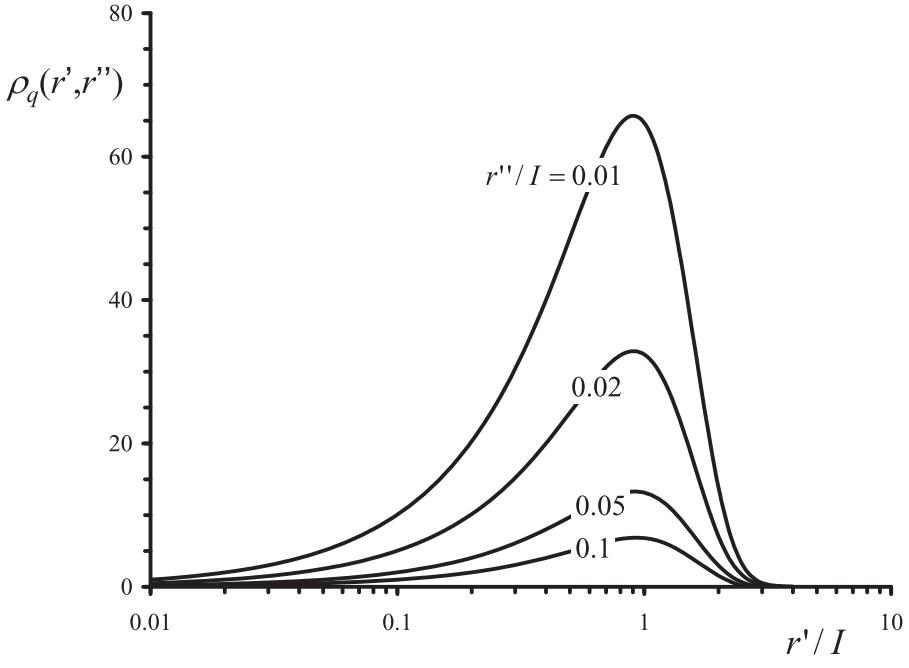

Figure 4. Correlation coefficient $\rho_q(r', r'')$ of the flux versus the distance $\frac{r'}{I}$ and different values of $\frac{r''}{I}$ (Gaussian autocorrelation of ε).

Dagan, 1999, Figure 4], it turned out that such an approximation becomes sufficiently accurate for $R \geq 5I$. Thus, our results cast in a more physically based context the numerical justification provided by *Indelman and Dagan* [1999] to their approximate expression of the velocity covariance.

[36] The function Ψ_q, as computed from the second expression of (31) and (53), is depicted in Figure 5. It is displayed versus the normalized radial distance $\frac{r}{I}$ from the well and some values of σ_ε^2. Because of its monotonic decrease with r, it results that $\Psi_q(\infty) \leq \Psi_q(r) \leq \Psi_q(0)$. In particular, the far-field limit is practically attained at a distance slightly larger than three integral scales. It is interesting to observe that the distortion effect because of the combination of the medium heterogeneity and the distance

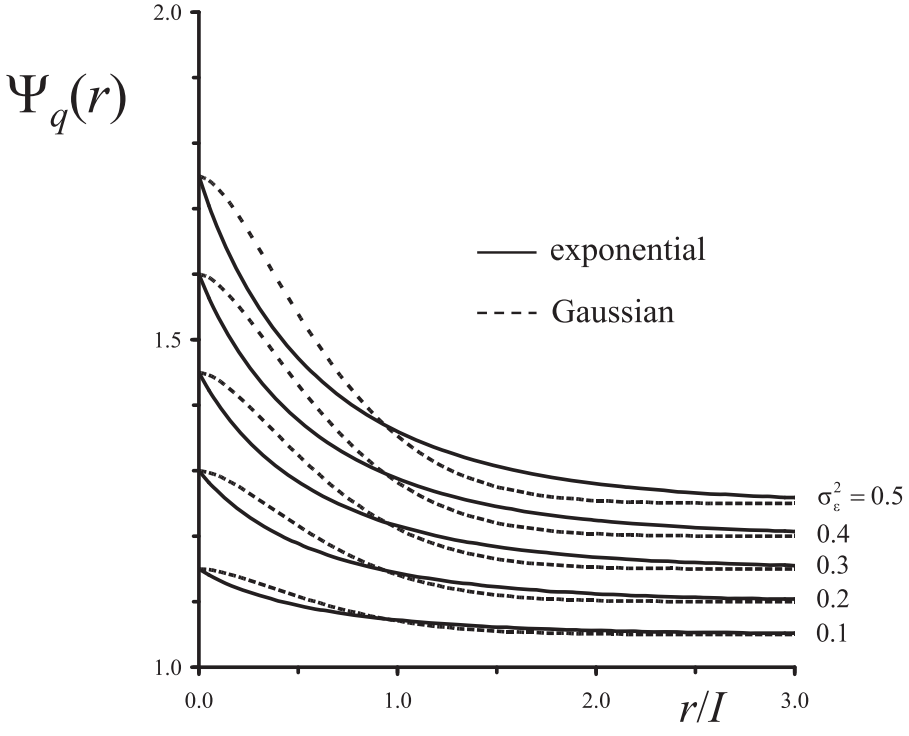

Figure 5. The characteristic heterogeneity function Ψ_q of the flux as function of the normalized radial distance $\frac{r}{I}$ and a few values of the variance σ_ε^2.

dependence is more sensitive for $r \leq I$. These properties of the function $\Psi_q(r)$ may be applicable in checking more involved numerical codes.

5.3. Equivalent Versus Apparent Transmissivity

[37] Both the equivalent and the apparent transmissivities vary with the distance from the well and, therefore, they are not local properties. In particular, they are bounded between the harmonic T_H and the geometric T_G mean. To study the transition from T_H to T_G, it is convenient to represent $T^{(\mathrm{eq})}$ and $T^{(\mathrm{ap})}$ as follows:

$$T^{(\alpha)}(r) = [1 - \omega^{(\alpha)}(r)]T_H + \omega^{(\alpha)}(r)T_G \quad (\alpha \text{ can be either eq or ap}), \tag{56}$$

where $\omega^{(\alpha)}(0) = 0$ and $\omega^{(\alpha)}(\infty) = 1$. In other words, the equivalent and the apparent transmissivities are weighted means of the harmonic and the geometric means. The weighting functions $\omega^{(\alpha)}$ depend upon the radial distance, and they are given by

$$\omega^{(\mathrm{eq})}(r) = 2\left(1 + \frac{\sigma_\varepsilon^2}{2}\right)\frac{1 - \psi_H(r)}{1 + \sigma_\varepsilon^2 \psi_H(r)},$$
$$\omega^{(\mathrm{ap})}(r) = 2\left(1 + \frac{\sigma_\varepsilon^2}{2}\right)\frac{1 - 2\psi_q(r)}{2 + \sigma_\varepsilon^2[1 + 2\psi_q(r)]}. \tag{57}$$

[38] In Figure 6, we have depicted (black lines) $\omega^{(\mathrm{eq})}$ for $\sigma_\varepsilon^2 = 0.5$ versus the normalized radial distance $\frac{r}{I}$ and some values of the parameter $\frac{\ell_0}{I}$. For comparison purposes, we have also depicted (red lines) the weight $\omega^{(\mathrm{ap})}$. Even if both $\omega^{(\mathrm{eq})}$ and $\omega^{(\mathrm{ap})}$ depend upon the position, it is seen that $\omega^{(\mathrm{ap})}$ is a more robust property. Such a result, which is in agreement with previous studies (an overview can be found in the work of *Dagan* [2001]), is because of the fact that the equivalent conductivity (unlike the apparent one) is defined via the mean head $\langle H \rangle_2$, and therefore it depends upon the additional parameter $\frac{\ell_0}{I}$ (see equations (18) and (34)). This drastically affects the rate of approaching the far-field value (i.e., T_G) of the equivalent transmissivity. In particular, $T^{(\mathrm{eq})} \simeq T_H$ for $\frac{r}{I} < 1$, whereas it slowly increases with $\frac{r}{I}$. Another important feature is that the rate of getting the asymptotic $T^{(\mathrm{eq})}(\infty)$ depends significantly upon the shape of ρ_ε. To explain this, it is worth recalling that the Gaussian ρ_ε model pertains to a continuous transmissivity field, whereas the exponential model is related to a discontinuous field, e.g., a formation made up by inclusions with jumps of the transmissivity values at the boundary between each inclusion [see, e.g., *Dagan,* 1989]. This lower-scale difference in the formation structure is more influential here because of the streamline's convergence at the well.

[39] The definition of equivalent transmissivity has implications in the analysis of the pumping tests. Indeed, equation (34) corresponds to the transmissivity value determined in a pumping test by an observer that measures the mean head for a fixed Q. Thus, if the transmissivity measurements are used in simulations as representative of T^{ef}, this is clearly underestimated. The discrepancy between transmissivity values determined by pumping tests and those to be used in regional-scale simulations has been recently tackled by *Dagan and Lessoff* [2007]. Similar to this study [see *Dagan and Lessoff*, 2007, Figure 6], they found that $T^{(\mathrm{eq})} \approx T_H$ for relatively large portions of the flow domain. Thus, the expression (56) serves to better quantify the problem of identifying the values of the transmissivity to be used when simulating well flows at regional scale.

6. Summary and Recommendations for Practical Applications

[40] This paper focuses on the statistical moments of the head and flux for steady flow toward a well. The fluctuation

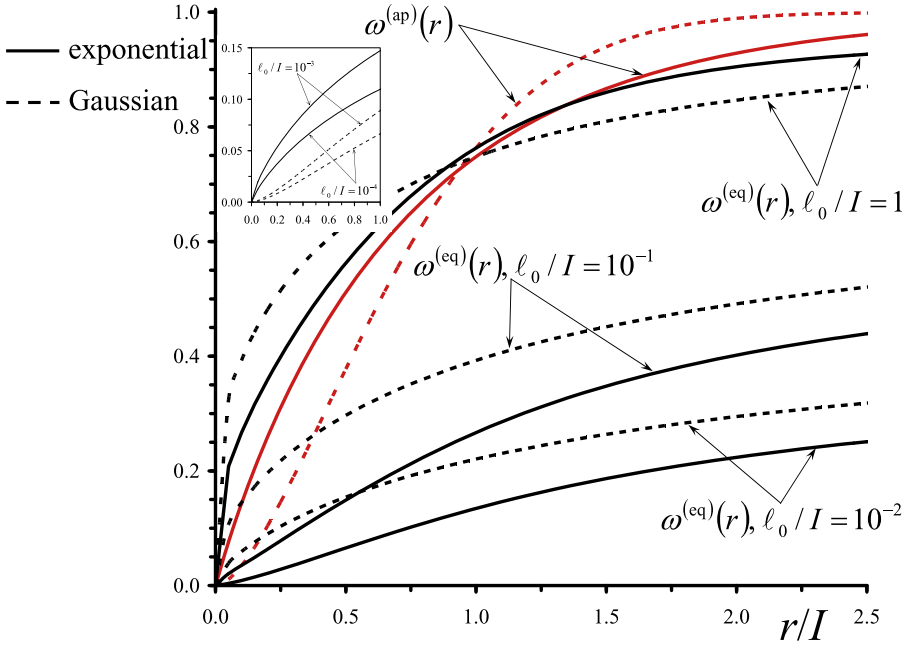

Figure 6. The dependence of the weights (equation (57)) $\omega^{(\mathrm{ap})}$ (red lines) and $\omega^{(\mathrm{eq})}$ (black lines) upon the dimensionless radial distance $\frac{r}{I}$ from the well.

(3) modeled as a stationary RSF with given variance σ_ε^2 and autocorrelation function ρ_ε. Moments are derived for any ρ_ε in terms of a few quadratures, which are easily (in some cases in a closed form) computed after specifying the shape of ρ_ε.

[41] The head variance σ_H^2 (and similarly for the flux variance) is singular at the well. This is explained by noting that the domain surrounding the well *de facto* behaves as a homogeneous unit with constant (equal to the harmonic mean) transmissivity. Unlike the previous study of *Dagan* [1982], who considered the near- and far-field behavior of σ_H^2, we analytically compute the head variance in the entire flow domain. This enables one to better quantify the range of applicability of the approximate solutions of *Dagan* [1982].

[42] The flux is expressed in a general form, which requires only one quadrature (that is analytically carried out for both exponential and Gaussian ρ_ε). Thus, the computational burden related to the involved multidimensional numerical quadratures [*Fiori et al.*, 1998; *Riva et al.*, 2001] is overcome. One interesting result (especially in view of the applications) is that the maximum uncertainty in the flux is achieved at the well (where $\mathrm{CV}_q = 2\sigma_\varepsilon$). This is understandable because of the high-velocity fluctuations there. Instead, far from the well (say, for $r > 10I$), it yields $\mathrm{CV}_q = \sqrt{\frac{5}{2}}\sigma_\varepsilon$, since velocity fluctuations (which are mainly addressed to the flow nonuniformity) are drastically reduced.

[43] We have analyzed the head autocorrelation $\rho_H(r', r'')$ at two different radial positions r' and r''. For $r'' \ll I$, the autocorrelation $\rho_H(r', r'')$ persists over large portions of the flow domain, whereas when $r'' \gg I$, it drastically reduces since the boundary condition does not impact anymore. A qualitatively similar behavior is observed when considering the autocorrelation $\rho_q(r', r'')$ of the flux. Besides being of theoretical interest, the statistical moments derived here may serve in some practical applications, such as the analysis of tracer tests.

[44] The (second-order) mean flux $\langle q_r(r)\rangle_2$ has been derived. It is represented as $\langle q_r(r)\rangle_2 = q^{(0)}(r)\Psi_q(r)$ to show how the medium heterogeneity modifies (through the distortion function Ψ_q) the homogeneous flux $q_r^{(0)}$. It is easy to establish both the near-field behavior, i.e., $\Psi_q(0) = 1 + \frac{3}{2}\sigma_\varepsilon^2$, and the far−field behavior, i.e., $\Psi_q(\infty) = 1 + \frac{\sigma_\varepsilon^2}{2}$. For exponential and Gaussian ρ_ε, the characteristic heterogeneity function $\Psi_q(r)$ is computed in closed form.

[45] Another advantage of the perturbation approach employed in this paper is that it leads to the localization of the flow equations [*Tartakovsky and Neuman*, 1998]. Thus, we have defined the equivalent transmissivity $T^{(\mathrm{eq})}$ as that pertaining to a homogeneous (fictitious) formation that conveys the same specific volumetric rate of the real formation. We have then compared such a definition with that of apparent transmissivity $T^{(\mathrm{ap})}$. In both the cases, we have obtained a simple general expression for $T^{(\mathrm{eq})}$ and $T^{(\mathrm{ap})}$. These properties vary with the distance from the well, i.e., they are not effective medium properties. Both $T^{(\mathrm{eq})}$ and $T^{(\mathrm{ap})}$ are weighted averages between the harmonic transmissivity T_H and the effective transmissivity T^{ef} in uniform flow.

[46] A salient question is whether it is possible to solve the flow equations "only once" by dealing with a homogeneous medium having the same hydraulic response of the actual one. It is well known that, under natural gradient conditions (i.e., uniform mean flow), such an upscaling is possible provided that one uses the geometric mean T_G. However, such a rule does not apply to a well-type flow, for which the upscaled transmissivity depends on the relative radial distance $\frac{r}{I}$ (Figure 6). To illustrate how the theoretical results can be used to tackle such a problem, we consider a hypothetical heterogeneous (with $\sigma_\varepsilon^2 = 0.5$) aquifer. Two avenues are, in principle, possible. First, one can use a Monte Carlo procedure regarding $Y(\mathbf{x}) = \ln T(\mathbf{x})$ as a normally distributed RSF. The Monte Carlo method has two limitations. Indeed, to generate the spatial distribution of the Y field in an accurate manner, the numerical grid has to be small compared to the integral scale (fine-scale simulation). This requirement may result in a very large system of equations. In addition, to capture the statistics of the dependent variables, a large number of realizations are needed (even when one is only interested in the mean values). At present, these two requirements are too demanding in most hydrological applications because of the heavy numerical burden. Furthermore, scarcity of field data and imprecision of measurements make even the identification of the T statistics quite uncertain. This intrinsic uncertainty reduces the ability of Monte Carlo simulations to produce accurate results, and thus may reduce the advantage of computationally intensive Monte Carlo simulations over simpler (although approximate) methodologies.

[47] As a second option, only one simulation with (properly assigned) nodal values of the transmissivity can be adopted. In such a case, the critical issue concerns the values to be assigned to each point of the flow domain. For instance, at $r \approx I$ it is seen (red line in Figure 6) that $\omega^{(\mathrm{ap})} \approx 0.75$. As a consequence, the effective transmissivity would result only for 75% equal to the geometric mean T_G, i.e., the value that one would (erroneously) use if approaching such a problem in the same manner as for mean uniform flows. By the same token, one can easily argue that even more dramatic are the consequences if one deals with smaller radial distances. Finally, it is also seen from Figure 6 that a largely variable (and therefore largely uncertain) value for the equivalent transmissivity should be considered (depending on the ratio $\frac{\ell_0}{I}$).

[48] While this simple example shows how these theoretical results can be readily applied to solve practical problems, there are many factors, the impact of which requires further investigation, e.g., high variance, influence of the aquifer boundaries, conditioning by transmissivity measurement, unsteady flow, quantifying the errors introduced by localization, etc. Hence, the subject calls for further research, although it should be realized that, in applications, the usefulness of refinements is limited by the lack of data and mainly by the imprecise characterization of the heterogeneous fine-scale structure.

Appendix A: Derivation of the Cross Covariance $C_{\varepsilon H}$

[49] In order to compute the covariances $C_{\varepsilon H}$ and C_{E_r}, we first calculate the head fluctuation. Thus, from (8) and using the relationship $\frac{\partial}{\partial x_m} = \frac{x_m}{x}\frac{d}{dx}$, one has

$$H^{(1)}(\mathbf{r}) = \frac{Q}{T_A}\int_\Omega \frac{d\overline{\mathbf{r}}}{(2\pi)^2}\varepsilon(\overline{\mathbf{r}})\,\frac{\overline{\mathbf{r}}\cdot(\overline{\mathbf{r}}-\mathbf{r})}{(\overline{r}|\overline{\mathbf{r}}-\mathbf{r}|)^2}. \tag{A1}$$

The cross covariance $C_{\varepsilon H}$ is calculated by multiplying $\varepsilon(\mathbf{r}')$ by (A1) evaluated in $\mathbf{r}'' \neq \mathbf{r}'$, and subsequently taking the expectation to get

$$C_{\varepsilon H}(\mathbf{r}',\,\mathbf{r}'') = \frac{Q}{T_A}\left(\frac{\sigma_\varepsilon}{2\pi}\right)^2\int_\Omega d\overline{\mathbf{r}}\rho(\overline{r})\,\frac{(\mathbf{r}'-\overline{\mathbf{r}})\cdot(\mathbf{r}'-\mathbf{r}''-\overline{\mathbf{r}})}{(|\mathbf{r}'-\overline{\mathbf{r}}|\,|\mathbf{r}'-\mathbf{r}''-\overline{\mathbf{r}}|)^2}. \tag{A2}$$

Switching to polar coordinates $\overline{\mathbf{r}} = \overline{\mathbf{r}}(\overline{r},\,\theta)$

$$C_{\varepsilon H}(r',\,r'') = \frac{Q}{T_A}\left(\frac{\sigma_\varepsilon}{2\pi}\right)^2\int_0^\infty d\overline{r}\overline{r}\rho(\overline{r}) \int_0^{2\pi} d\theta\frac{\overline{r}^2 + r'(r'-r'') - \overline{r}(2r'-r'')\,\cos\theta}{\beta(r')\,\beta(r'-r'')}, \tag{A3}$$

$$\beta(a) = \overline{r}^2 + a^2 - 2a\overline{r}\cos\theta. \tag{A4}$$

Integrating over the angle

$$\int_0^{2\pi} d\theta\frac{\overline{r}^2 + r'(r'-r'') - \overline{r}(2r'-r'')\,\cos\theta}{\beta(r')\,\beta(r'-r'')} = 2\pi\frac{h(\overline{r}-|r'-r''|) - h(r'-\overline{r})}{\overline{r}^2 - r'(r'-r'')} \tag{A5}$$

(the h function has been defined in section 3.1), and substituting into (A3), leads to (11).

[50] **Acknowledgments.** This study was supported by grants from Programma di scambi internazionali per mobilita di breve durata, Naples University (Italy), and MIUR 2007 WA23ZC. The author is very grateful to the Associate Editor and to the three anonymous reviewers for their thorough and helpful comments, which have significantly improved the early version of the manuscript. Suggestions from Gabriella Pisanti are kindly acknowledged.

References

Ababou, R., and E. F. Wood (1990), Comment on "Effective groundwater model parameter values: Influence of spatial variability of hydraulic conductivity, leakance and recharge" by, J. J. Gomez-Hernandez and S. M. Gorelick, *Water Resour. Res.*, *26*, 1643–1846, doi:10.1029/90WR01965.

Butler, J. J. (1991), A stochastic analysis of pumping tests in laterally nonuniform media, *Water Resour. Res.*, *27*, 2401–2414, doi:10.1029/91WR01371.

Dagan, G. (1982), Stochastic modeling of groundwater flow by unconditional and conditional probabilities. 1. Conditional simulation and the direct problem, *Water Resour. Res.*, *18*, 813–833, doi:10.1029/WR018i004p00813.

Dagan, G. (1989), *Flow and Transport in Porous Formations*, Springer, New York.

Dagan, G. (2001), Effective, equivalent, and apparent properties of heterogeneous media, in *Mechanics for a New Millennium*, edited by H. Aref and J.W. Philips, pp. 473–486, Kluwer Acad., Dordrecht, Netherlands.

Dagan, G., and S. C. Lessoff (2007), Transmissivity upscaling in numerical aquifer models of steady well flow: Unconditional statistics, *Water Resour. Res.*, *43*, W05431, doi:10.1029/2006WR005235.

Dagan, G., S. C. Lessoff, and A. Fiori (2009), Is transmissivity a meaningful property of natural formations? Conceptual issues and model development, *Water Resour. Res.*, *45*, W03425, doi:10.1029/2008WR007410.

Desbarats, A. J. (1992), Spatial averaging of transmissivity in heterogeneous fields with flow toward a well, *Water Resour. Res.*, *28*, 757–767, doi:10.1029/91WR03099.

Fiori, A., P. Indelman, and G. Dagan (1998), Correlation structure of flow variables for steady flow toward a well with application to highly anisotropic heterogeneous formations, *Water Resour. Res.*, *34*, 699–708, doi:10.1029/97WR02491.

Gomez-Hernandez, J. J., and S. M. Gorelick (1989), Effective groundwater model parameter values: Influence of spatial variability of hydraulic conductivity, leakance and recharge, *Water Resour. Res.*, *25*, 405–419, doi:10.1029/WR025i003p00405.

Guadagnini, A., and S. P. Neuman (1999), Nonlocal and localized analyses of conditional mean steady state flow in bounded, randomly nonuniform domains., 1. Theory and computational approach, *Water Resour. Res.*, *35*, 2999–3018, doi:10.1029/1999WR900160.

Guadagnini, A., M. Riva, and S. P. Neuman (2003), Three-dimensional steady state flow to a well in a randomly heterogeneous bounded aquifer, *Water Resour. Res.*, *39*(3), 1048, doi:10.1029/2002WR001443.

Indelman, P. (2001), Steady-state flow in heterogeneous porous media, *Transp. Porous Media*, *45*, 105–127.

Indelman, P., and B. Abramovich (1994), Nonlocal properties of nonuniform averaged flows in heterogeneous media, *Water Resour. Res.*, *30*, 3385–3393, doi:10.1029/94WR01782.

Indelman, P., and G. Dagan (1999), Solute transport in divergent radial flow through heterogeneous porous media, *J. Fluid. Mech.*, *384*, 159–182.

Indelman, P., and V. Zlotnik (1997), Average steady nonuniform flow in stratified formations, *Water Resour. Res.*, *33*, 927–934, doi:10.1029/97WR03790.

Indelman, P., A. Fiori, and G. Dagan (1996), Steady flow toward wells in heterogeneous formations: Mean head and equivalent conductivity, *Water Resour. Res.*, *32*, 1975–1983, doi:10.1029/96WR00990.

Lifshitz, I. M., and L. H. Rozentsveig (1946), On the theory of polycrystal elastic properties, *J. Exp. Theor. Phys.*, *16*, 967–980.

Matheron, G. (1967), *Elements Pour Une Theorie des Milieux Poreux*, Masson et Cie, Paris.

Muskat, M. (1937), *The Flow of Homogeneous Fluids Through Porous Media*, McGraw-Hill, New York.

Naff, R. L. (1991), Radial flow in heterogeneous porous media: an analysis of specific discharge, *Water Resour. Res.*, *27*, 307–316, doi:10.1029/90WR02410.

Neuman, S. P., and S. Orr (1993), Prediction of steady state flow in nonuniform geologic media by conditional moments: Exact nonlocal formalism, effective conductivities, and weak approximation, *Water Resour. Res.*, *29*, 341–364, doi:10.1029/92WR02062.

Neuman, S. P., and P. A. Witherspoon (1969), Theory of flow in a confined two aquifer system, *Water Resour. Res.*, *5*, 803–814, doi:10.1029/WR005i004p00803.

Oliver, D. S. (1993), The influence of nonuniform transmissivity and storativity on drawdown, *Water Resour. Res.*, *29*, 169–178, doi:10.1029/92WR02061.

Riva, M., A. Guadagnini, S. P. Neuman, and S. Franzetti (2001), Radial flow in a bounded, randomly heterogeneous aquifer, *Transp. Porous Media*, *45*, 139–193.

Rubin, Y. (2003), *Applied Stochastic Hydrogeology*, Oxford Univ. Press, New York.

Sanchez-Vila, X. (1997), Radially convergent flow in heterogeneous porous media, *Water Resour. Res.*, *33*, 1633–1641, doi:10.1029/97WR01001.

Severino, G., A. Santini, and A. Sommella (2008), Steady flows driven by sources of random strength in heterogeneous aquifers with application to partially-penetrating wells, *Stochastic Environ. Res. Risk Assess.*, *22*, 567–582, doi:10.1007/s 00477-007-0175-5.

Schad, H., and G. Teutsch (1994), Effects of the investigation scale on pumping test results in heterogeneous porous aquifers, *J. Hydrol.*, *159*, 61–77.

Shvidler, M. I. (1966), The source-type solution of the problem of unsteady flow in random porous media, *Fluid Dyn.*, *1*(4), 95–98.

Shvidler, M. I. (1985), *Stochastic Hydrodynamics of Porous Media*, Nedra, Moscow.

Tartakovsky, D. M., and S. P. Neuman (1998), Transient flow in bounded randomly heterogeneous domains. 2. Localization of conditional mean equations and temporal nonlocality effects, *Water Resour. Res.*, *34*, 13–20, doi:10.1029/97WR02117.

Tartakovsky, D. M., A. Guadagnini, F. Ballio, and A. M. Tartakovsky (2002), Localization of mean flow and equivalent transmissivity tensor for bounded randomly heterogeneous aquifers, *Transp. Porous Media*, *49*, 41–58.

G. Severino, Division of Water Resources Management, University of Naples FEDERICO II, via Universitá 100, 80055, Portici, Italy. (gerardo.severino@unina.it)